INTEGRAL OBSERVATIONS OF SS433: ANALYSIS OF PRECESSIONAL AND ORBITAL X-RAY PERIODICITIES

A.M. Cherepashchuk[1], R.A. Sunyaev[2], E.V. Seifina[3], E.A. Antokhina[3], D.I. Kosenko[3], S.V. Molkov[4], N.I. Shakura[5], K.A. Postnov[5], A.N. Timokhin[5], and I.E. Panchenko[5]

[1] *Sternberg Astronomical Institute, Universitetsky pr. 13, 119992, Moscow, Russia*
[2] *Space Research Institute, Russian Academy of Sciences, Profsoyuznaya 84/32, 117810 Moscow, Russia*
[2] *Max-Planck-Institute für Astrophysik, Karl-Schwarzschild-Str. 1, D-85740 Garching bei München, Germany,*
[3] *Sternberg Astronomical Institute, Universitetsky pr. 13, 119992, Moscow, Russia*
[4] *Space Research Institute, Russian Academy of Sciences, Profsoyuznaya 84/32, 117810 Moscow, Russia*
[5] *Sternberg Astronomical Institute, Universitetsky pr. 13, 119992, Moscow, Russia*

ABSTRACT

Hard X-ray *INTEGRAL* observations of SS 433 carried out during 2003-2005 years are presented. Analysis of precessional and orbital variability is presented. The width of X-ray eclipse in the $25-50$ keV range at the precessional phase $\psi = 0.1$ (accretion disk is open to observer) is higher than that in the Ginga $18.4-27.6$ keV range. This fact suggests existance the presence of hot extended corona around the supercritical accretion disk. Spectrum of hard X-rays in the range $10-200$ keV does not change with the precessional phase which also suggests that hard X-ray flux is generated in the hot extended corona around the accretion disk. The parameters of this hot corona are: $kT = 23-25$ keV, $\tau = 1.8-2.8$. Mass ratio estimated from the analysis of the ingress part of the eclipse light curve is in the range $q = m_x/m_v = 0.3-0.5$.

1. INTRODUCTION

SS 433 is a massive eclipsing X-ray binary with precessing supercritical accretion disk and relativistic jets. Narrow collimated relativistic jets ($v = 0.26c$) are precessing with the period $P_{prec} = 162^d.5$. Orbital period is $13^d.08$ ([1]). There are problems with optical classification of the determination of its radial velocity curve ([2], [3], [4], [5], [6]). This unique X-ray binary at an advanced evolutionary stage has been investigated in optical, radio and X-ray ranges (see review of Fabrika [7] and references therein).

First *INTEGRAL* observations of SS 433 in hard X-rays gave a surprise: SS 433 is a hard X-ray source with emission clearly detected up to 100 keV. We concluded that SS 433 is a supercritical microquasar with hard X-ray spectrum ([8]). SS 433 was observed by *INTEGRAL* in A01-A03 from 2003 to 2005.

2. OBSERVATIONS AND DATA REDUCTION

In this work all publically avaliable data on SS 433 obtained by *INTEGRAL* from March, 2003 to November, 2004 (AO-1,2) and the results of our pointed observations at October 12-22, 2005 (AO-3) are presented.

The data reduction was performed by the Offline Science Analysis (OSA) software version 5.1, developed by the *INTEGRAL* science data center (ISDC, http://isdc.unige.ch [9]).

The light curves where reconstructed by processing all the available observations, obtained by the ISGRI/IBIS detector in the $25-50$ keV energy band. The light curve points where taken from the mosaic images integrated by each 10 ScW (Science Windows) with a standard background approximation procedure. Thus, a typical exposition time for each light curve point is ~ 20 ksec.

The variability analysis is based on the precessional and orbital ephemeris of SS 433 by [7]. The orbital minima:

$$JD_{MinIHe} = 2450023.62 + 13.08211 * E$$

and the maximal emission lines separation T_3 moments:

$$JD_{T3} = 2443507.47 + 162.375 * E1,$$

where E and $E1$ are the orbital and precession cycle numbers respectively.

During the 3 years of *INTEGRAL* observations (2003-2005) cover a wide range of the precession phases of SS 433 . The three observation sets of AO-1 are performed at $\psi = 0.72-0.88$ (incontiunosly), $0.95-0.1$ (continuosly); AO-2: $\psi = 0.0-0.15$ (incontinuously), $0.22-0.23$ (continuously), $0.33-0.35$ (continuously); AO-3: $\psi = 0.5-0.56$. The time distribution of these observations is displayed in Fig.1. The T_3 moments are indicated by squares and the closest orbital minima – by triangles.

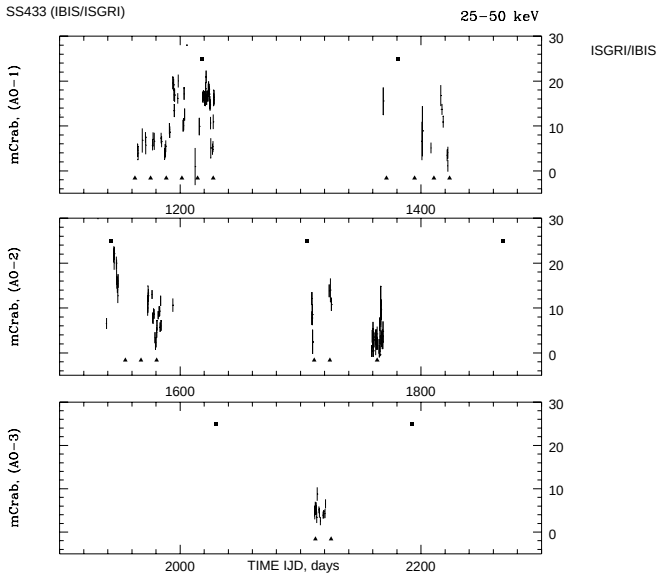

Figure 1. Observations of SS 433 in $2003 - 2005$*. The squares indicate the precessional face-on (T_3) moments, and the triangles indicate the orbital minima. The units of the horizontal axis are* $IJD = JD - 2451544.5$*.*

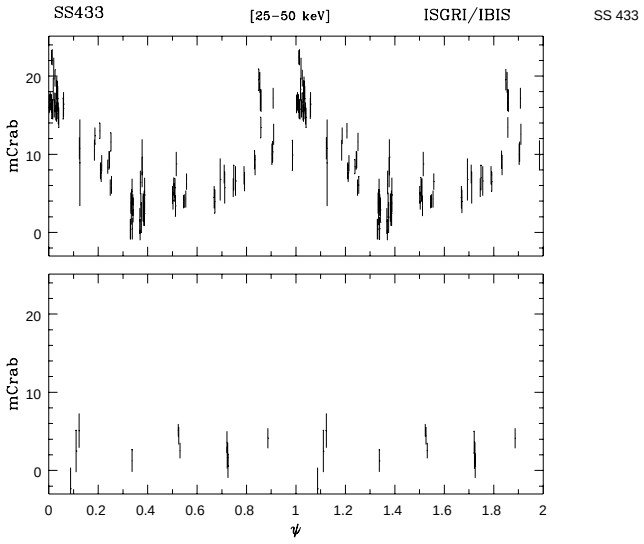

Figure 2. Precessional light curves of SS 433 . The upper panel: maximum flux outside of eclipses; the bottom panel: minimum flux at the middle of eclipses

3. PRECESSIONAL VARIABILITY

The $25 - 50$ keV light curve composed from all the available ISGRI/IBIS observations of SS 433 folded with the precessional period $P_{prec} = 162^d.5$ is displayed in Fig. 2.

The face-on disk position (T_3) defined as the maximim of the optical emission lines separation is taken as the moment of zero precession phase. The upper and lower panels of Fig. 2 display the X-ray flux (mCrabs) out of eclipse of the X-ray source by the normal star and in the middle of the eclipse, respectively.

Fig. 2 shows that the flux out of eclipse varies from 3 mCrab (crossover phase) to 18 mCrab (T_3 phase). The flux in the middle of eclipse (primary minimum) has no significant variablity, staying on average at a level of 2.9 mCrab.

4. ORBITAL ECLIPSE VARIABILITY

Fig. 3 displays the shape of the eclipses of SS 433 X-ray source by the normal component in the energy band $25 - 50$ keV observed in different precession phases ψ. The eclipse at $\psi = 0.1$ is obtained by folding all the available light curves in the phase interval $\psi = 0.95 - 0.15$ (JD 2452770-2453270).

The eclipse depth is maximal at $\psi = 0.1$ and decreases with the phase of precession. This is clearly seen for individual eclipse light curves for $\psi = 0.22, 0.34$ (first crossover), $\psi = 0.5, 0.72$ (some later than the second crossover), and 0.88 (see Fig. 3). The dotted line in the figure indicates the moments of the primary minimum.

The good correspondence between X-ray minima with the optical ephemeris for the precession phases close to T_3 as well as the delay of the X-ray light curve with respect to the optical one at $\psi \sim 0.5$ should be specially noted.

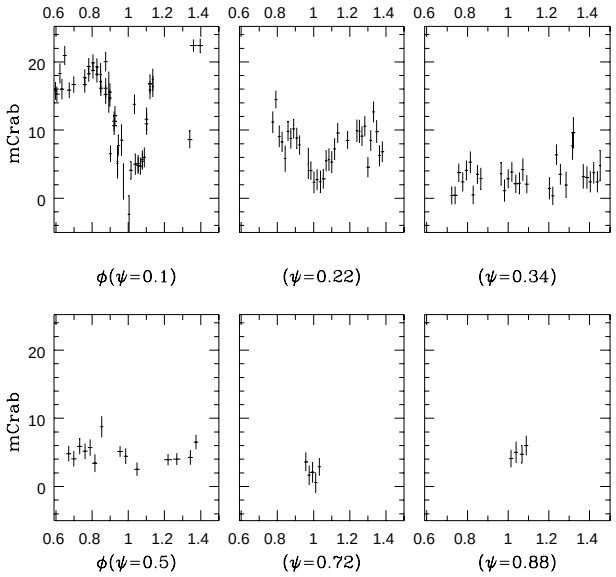

Figure 3. Orbital light curves of SS 433 in different phases ψ of precession.

Table 1. Parameters of the SS433 spectrum for CompPS model

Model	kT (keV)	τ_y	H/R	Normalization	Reduced χ^2
hemisphere	24.9 ± 7.7	1.8 ± 0.6	–	13.3 ± 3.8	1.08 (5 d.o.f.)
slab	23.2 ± 6	2.8 ± 0.6	0.5	12.7 ± 4.5	1.06 (5 d.o.f.)

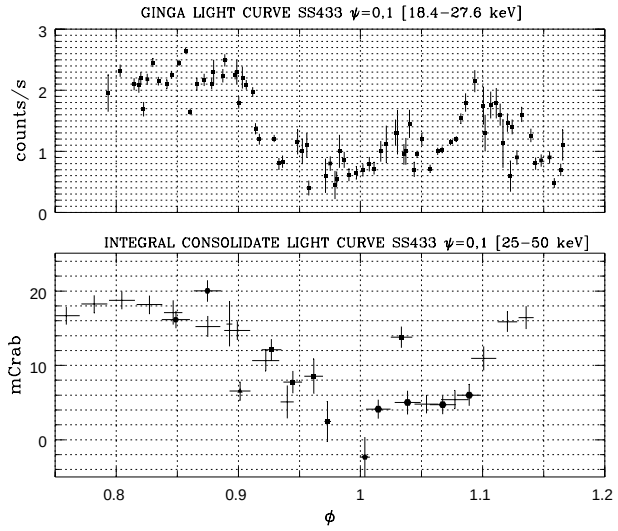

Figure 4. The eclipse shape at $\psi = 0.1$

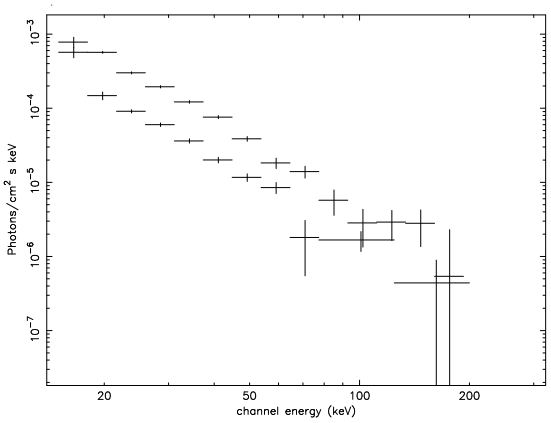

Figure 5. The IBIS/ISGRI $10-200$ keV high and low state SS 433 spectra (upper and lower points, respectively).

5. ECLIPSE IN THE PHASE $\psi = 0.1$

Fig. 4 displays the eclipse light curves in the $25 - 50$ keV band obtained by *INTEGRAL* in comparison with the $18.4 - 27.6$ keV light curves obtained by Ginga ([10]), denoted below as hard and soft bands.

Evidently, the eclipse width in the hard band is greater than in the soft one. This seems unexpected because such a behaviour is opposite to what is observed in most X-ray binaries where the X-ray eclipse width gets smaller in harder bands.

The ascending part of the eclipse in the Ginga data is disturbed, probably, by the light absorption by the accretion flows. Some distortions at the same phases can be also noticed in the hard band data. The phase of the excess point inside the eclipse is coincident with the local maximum on the Ginga light curve.

To avoid the influence of the accretion flows, we analyze only the descending part of the eclipse, which can be considered as corresponding to the pure geometrical eclipse by the opaque body of the optical component.

6. SPECTRAL ANALYSIS

For spectral analysis, we separated all available observations into two parts: with the X-ray flux below the mean value (around 10 mCrab in the 20-50 keV energy range) and above it. The spectra where obtained using the software developed by [11] (IKI RAS). No significant difference in the spectral shape was found (see Fig. 5). This suggests a fairly broad region emitting in hard X-rays with size comparable to that of the accretion disk, since (apart from orbital eclipses) the observed flux varies due to precession of the disk. The spectral shape of this region in the 20-100 keV range can be fitted by thermal comptonization model (CompPS, [12]). Equally good fits were found for two geometries of the emitting region: (1) a hemisphere with temperature $kT = 25 \pm 8$ keV and optical thickness for electron scattering $\tau_y = 1.8 \pm 0.6$, and (2) a slab with $kT = 23 \pm 6$ keV and $\tau_y = 2.8 \pm 0.6$ (see Fig. 6 and Table 1). In both cases the inclination angle is assumed to be 60 degrees. A blackbody component with $kT_{bb} = 1.8$ keV is added to slightly improve the fits.

This analysis suggests in addition to thermal X-ray emission from jets (which dominates at smaller energies in the standard X-ray band, see [13] and references therein for earlier works), the presence of an extended hot corona emitting in hard X-ray exists in SS433 around jets first discovered by *INTEGRAL* (Cherepashchuk et al [8], [5]). From the joint analysis of the X-ray orbital eclipses and precessional variability presented in this paper it follows that the size of the corona must be comparable with that of the accretion disk ($10^{11} - 10^{12}$ cm). The spectral fits presented above suggests the electron denisty around 10^{12} cm^{-3}. We note that such a density is indeed expected in the wind outflowing from a supercritical accretion disk with $\dot{M} \sim 10^{-4}$ M$_\odot$/yr and $v \sim 3000$ km/s at distances $\sim 10^{12}$ cm from the central source where

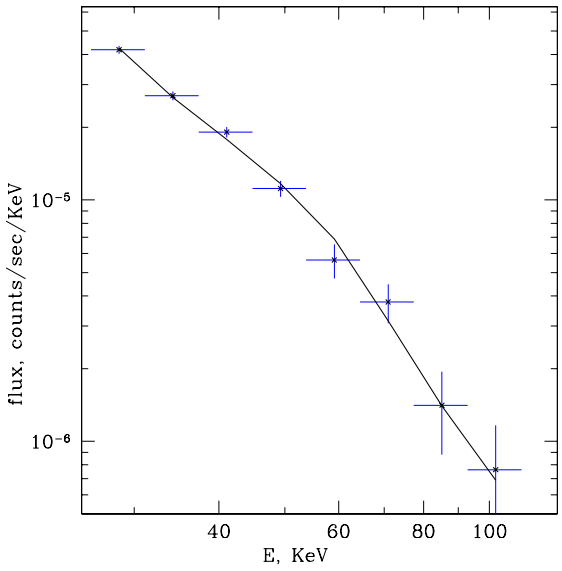

Figure 6. The IBIS/ISGRI $10-200$ *keV spectrum of SS 433 433 and its best fit by thermal comptonization model CompPS with slab geometry (solid line).*

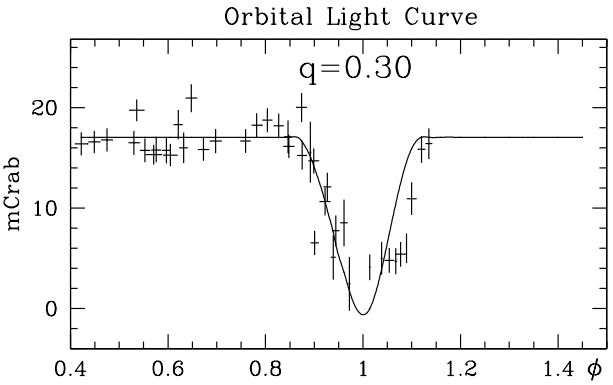

Figure 7. Eclipse fit for the mass ratio $q = 0.3$.

the photosphere should be formed. The heating of such a corona up to 25 keV can be due to violent interaction of mildly relativistic jets with the surrounding dense wind ([14]).

7. ANALYSIS OF ORBITAL AND PRECESSIONAL VARIABILITY

We carried out the joint analysis of orbital eclipses (ingress only) at the precessional phase $\psi_{prec} \sim 0.1$ and of the precessional light curve itself.

For the analysis of X-ray variability we used a geometrical model of SS433 utilized earlier to studies of the Ginga data [15] and the *INTEGRAL* X-ray light curve [5]. In this model, the binary system consists of an opaque "normal" star shaped by the Roche equipotential surface and a relativistic object surrounded by an optically and geometrically thick "accretion disk". The size of the "normal" star is determined by the sizes of the critical Roche lobe for the mass ratio $q = M_x/M_v$ (here M_x is the mass of the relativistic object).

The "accretion disk" includes the disk itself and an extended photosphere formed by the outflowing wind. The disk is inclined with respect to the orbital plane by the angle 20.30^o. The opaque disk body with a central cone-like region (funnel) is described by the radius r_d and the cone opening angle ω. The accretion disk radius is limited by the distance r_d from its center to the inner Lagrangian point. The relativistic object is surrounded by a transparent homogeneously emitting spheroid with the visible radius r_j and height b_j, which could be interpreted as a "corona" or a "thick jet" (without any relativistic motion).

Only the hot "corona" is assumed to emit hard X-ray flux, while the star and the opaque disk eclipse it during orbital and precessional motion. Physically, such a "corona" could be thought of as hot low-density plasma filling the funnel around the relativistic jets.

During precessional motion, the inclination of the disk with respect to the observer changes, causing different conditions of the "corona" visibility. The observed precessional variability can thus be used to obtain a "vertical" scan of the emitting structure, restricting the height b_j and the cone opening angle ω. The orbital variability (eclipses) allows one to scan the emitting structure "horizontally", rectricting the possible values of r_d, r_j, ω and the mass ratio q.

The results of the joint analysis of the orbital and precessional variabilities can be summarized as follows.

1). In the framework of our geometrical model of the hard X-ray emitting region in SS433, the eclipse shape (ingress) and the precessional amplitude of the hard X-ray light curve are best reproduced by a wide oblate "corona" located above an optically thick accretion disk.

2). At any q, the best fits for the observed wide orbital eclipse ($\psi_{prec} \sim 0.1$) are obtained for large visible radii of the hot corona r_j just slightly smaller than the disk radius r_d ($r_j/r_d = 0.7-0.9$). The height of the "corona" b_j is about $0.3-0.6$ of r_d and the cone opening angle is $\omega = 70-80^o$.

3). The precessional light curve taken alone does not restrict the binary mass ratio q: equally good fits are found for q varying from 0.05 to 1.0.

4). Analysis of the orbital X-ray eclipse ingress only (observed at $\psi_{prec} \sim 0.1$) shows that in the range of $q = 0.1-0.6$ the fit accuracy varies by some 10% only.

5). Simultaneous analysis of both precessional and orbital variability of SS433 allows one to constrain q to the range $0.3-0.5$. The fit is illustrated in Fig. 7 and Fig. 8.

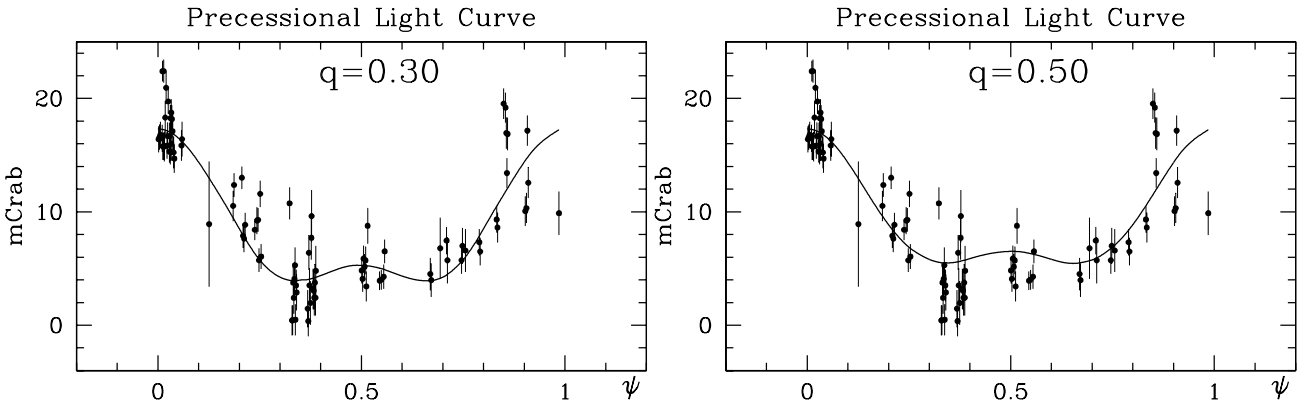

Figure 8. Precessional light curve fits for $q = 0.3$ and 0.5 (left and right panels, respectively).

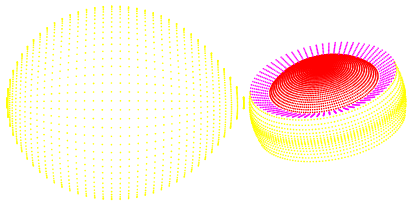

Figure 9. The graphical scheme of the emitting regions

8. CONCLUSIONS

Most probably, SS 433 contains a black hole. The detection of a hot extended corona around the supercritical accretion disk in SS 433 is a new result.

The future prospects are connected with a high resolution optical spectroscopy of SS 433 at the face-on disk phase (the planned Subaru observations). The new hard X-ray eclipse observations at $\psi = 0 - 0.1$ will be used to confirm the growth of the eclipse width with the photon energy, which directly evidences for the presence of an extended hot corona around the disk. The peculiarities of the ascending side of the eclipse are to be studied. These tasks are planned to be done by the *INTEGRAL* observations in May 2007.

ACKNOWLEDGMENTS

This work was partially supported by RFBR grants 06-02-16025 and 05-02-17489.

REFERENCES

[1] Goranskii, V.P., Esipov, V.F., Cherepashchuk, A.M., 1998, Astron. Reports, **42**, 209

[2] Gies, D.R., Huang, W., McSwain, M.V., 2002, ApJ **578**, L67

[3] Hillwig, T.C., Gies, D.R., Huang, W., et al 2004, ApJ **615**, 422

[4] Cherepashchuk, A.M.Sunyaev, R.A., Fabrika, S.N. et al, 2004 Proceedings of the 5th *INTEGRAL* Workshop on the *INTEGRAL* Universe (ESA SP-552). 16-20 February 2004, Munich, Germany. Scientific Editors: V. Schönfelder, G. Lichti & C. Winkler, p.207

[5] Cherepashchuk, A.M., Sunyaev, R.A., Fabrika, S.N., Postnov, K. A., Molkov, S. V., et al, & Aph. 2005, **437**, 561

[6] Barnes, A.D., Casares, J., Charles, P.A., Clark, J.S., Cornelisse, R., Knigge, C., Steeghs, D., 2005, MNRAS, (astro-ph/0510448)

[7] Fabrika, S.N., 2004, Astrophys. Space Phys. Rev. **12**, 1

[8] Cherepashchuk, A.M., Sunyaev, R.A., Seifina, E.V., Panchenko, I. E., Molkov, S. V., Postnov, K. A. 2003, Astron. & Aph. **411**, L441

[9] Courvoisier T.J.-L., Beckmann V., Bourban G., et al. 2003, Astron. & Aph., **411**, L53

[10] Kawai N. and Matsuoka M., 1989, Publ. Astron. Soc. Japan, **41**,491

[11] Revnivtsev M.G., Sunyaev R.A., Varshalovich D.A et al., PaZh, 2004 **30**, 430

[12] J. Poutanen, R. Svensson, 2006, ApJ, **470**, 249

[13] Filippova, E., Revnivtsev, M., Fabrika., S., Postnov, K., Seifina, E. 2006, Astron. & Aph., in press. astro-ph/0609367

[14] Begelman, M.C., King, A.R., Pringle, J.E. 2006, MNRAS, **370**, 399

[15] Antokhina, E.A., Seifina, E.V., Cherepashchuk, A.M., 1992, Astron. Zh, **69**, 282